STUDIES OF η AND η' MEASUREMENTS WITH THE TIME OF FLIGHT SPECTROMETER AT COSY*

E. RODERBURG

IKP I, Forschungszentrum Jülich, Germany

for
the COSY-TOF Collaboration
[R. Bilger[f], H. Brand[a], S. Brand[a], H. Clement[f], M. Dahmen[d], P. Cloth[d], V. Drüke[d], W. Eyrich[c], H. Freiesleben[b], D. Filges[d], P. Jahn[d], K. Kilian[d], M. Kirsch[c], H. Koch[a], R.A. Kraft[c], J. Krug[a], E. Kuhlmann[a], S. Lange[a], H. Machner[d], H. Matthäy[a], P. Michel[e], K. Möller[e], H.P. Morsch[d], C. Nake[d], B. Naumann[e], L. Naumann[e], W. Oelert[d], N. Paul[d], P. Ringe[a], E. Roderburg[d], K. Röhrich[d], A. Röser[a], M. Rogge[d], G. Schmidt[e], M. Schmidt[c], T. Sefzick[d], M. Steinke[a], F. Stinzig[c], V. Stobik[d], R. Stratmann[d], P. Turek[d], S. Wirtz[c]
[a]Univ. Bochum, [b] Techn. Univ. Dresden [c]Univ. Erlangen, [d] IKP-KFA Jülich, [e] ZFK Rossendorf, [f]Univ. Tübingen]

(Received August 24, 1993)

The Time of Flight Spectrometer offers the possibility to measure charged particles with a 4π acceptance. By measuring the two protons of the reaction $pp \rightarrow pp\eta(\eta')$ or the ^{3}He of the reaction $pd \rightarrow {}^3\mathrm{He}$, $\eta(\eta')$ the $\eta(\eta')$ can be detected in the missing mass distribution. These measurements will cover momenta and scattering angles which have not been measured up to now.

PACS numbers: 14.40. Aq, 24.85. +p

1. Introduction

The Time of Flight Spectrometer (TOF) is realized by a collaboration of about 50 physicists led by P. Turek. The involved institutes are : The universities of Bochum, Erlangen and Tübingen and the research centers

* Presented at the Meson-Nucleus Interactions Conference, Cracow, Poland, May 14-19, 1993.

of Jülich and Rossendorf. The Time of Flight Spectrometer will be situated at an external beam line of the Cooler Synchrotron (COSY) and it will have an acceptance of 4π for charged particles. There are three accepted proposals for measurements with the TOF - spectrometer: Proton-Proton-Bremsstrahlung, η, η' production and interaction, and associated strangeness production. This report follows the main lines of the η proposal.

In addition to the TOF–spectrometer the full spectrum of η-physics will be covered at COSY: At the internal target experiment COSY 11 [1] the threshold-behavior of the fundamental reaction $pp \to pp\eta(\eta')$ can be studied with good resolution. At the second internal target experiment — the Zero Degree Facility [2] - η production by proton impacts on nuclear targets will be measured. The η-measurements with the TOF - spectrometer are the topic of this report, further there are plans to measure the fusion reaction with the magnetic spectrometer BIG KARL which will be equipped with a Germanium Detector [3] in the entrance region.

2. Apparatus

The idea is to enclose the interaction point in an evacuated vessel, whose walls are covered with scintillators. The time of flight of each particle is measured and the full kinematics of each event can be reconstructed by assuming the masses of the particles.

As this is a fixed target experiment, the particles get a lorentz-boost in the forward direction, the best adapted form of the scintillators is a closed barrel, with the target placed in the entrance part. The most convenient form to get a circular endcap and a cylindrical surface can be reached with scintillators in the form of archimedian spirals, they naturally will cover a circular area and they offer the possibility for an inner beam hole which affects each scintillator in the same way. A layer of left curved scintillators is combined with a layer of right curved, to prohibit non resolvable patterns of multi-hit events a third layer of wedge-formed scintillators is added. In addition to the circular form two more advantages of this shape exist:

- the area of the pixels is proportional to the distance to the center.
- with reference to the light guiding view the scintillators (spirals and wedges) have cross-sections which grow in the direction of the photomultiplier. This causes an optimal light guiding behavior.

The endplate of the barrel is divided in an inner part - the quirl- with a radius of 58 cm and an outer part - the ring - with a radius from 57 cm to 154 cm. The pixels formed by the coincidence of three layers can be seen in Fig. 1.

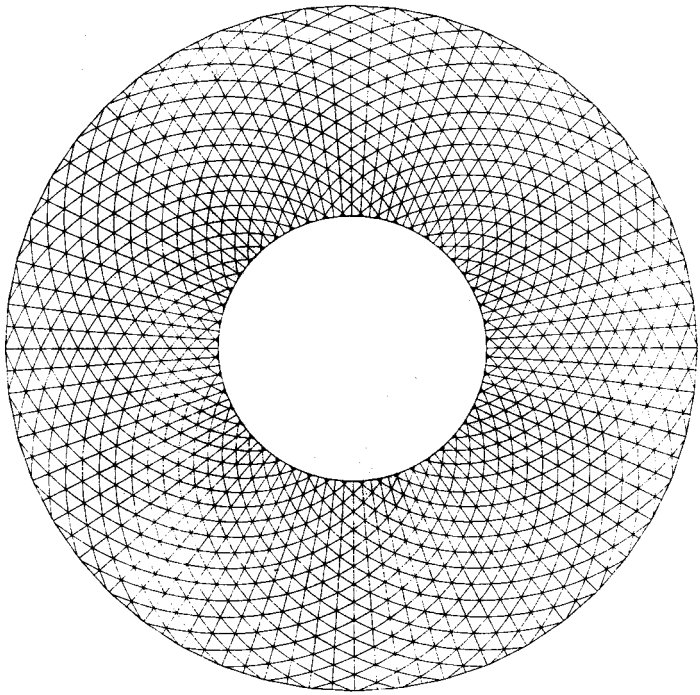

Fig. 1. Scintillators of the Ring

With 96 scintillators the quirl defines 1050 pixels, the ring with 192 scintillators 2304 pixels. The quirl has been operated successfully at JETSET (LEAR) and at PROMICE (CELSIUS).

The barrel is divided into three parts each of 2.5 m length. For each barrel-section 48 left, 48 right curved and 96 straight scintillator slabs are foreseen. This is a smooth extension from the endcap to the surface of the cylinder.

The target is described by C. Nake in these proceedings. It is optimized to provide very small liquid hydrogen or deuterium cells (in the order of cubic millimeter) with extremely small windows (few micrometer thickness).

The scintillator barrel defines the stop signal, it offers a huge space for counters in the entrance region which define the start signal. There exists a set of semiconductors and scintillators for defining the delayed trigger of Λ decay, they are built at the university of Erlangen. An arrangement of very thin start scintillators is developed at the Forschungszentrum Rossendorf, this is optimized for the Bremsstrahlung experiment.

For the first stage of η-measurements, especially the fusion measurement, we plan to use a miniature drift chamber — the induction drift chamber — in order to improve the ^{3}He track resolution [Fig. 2].

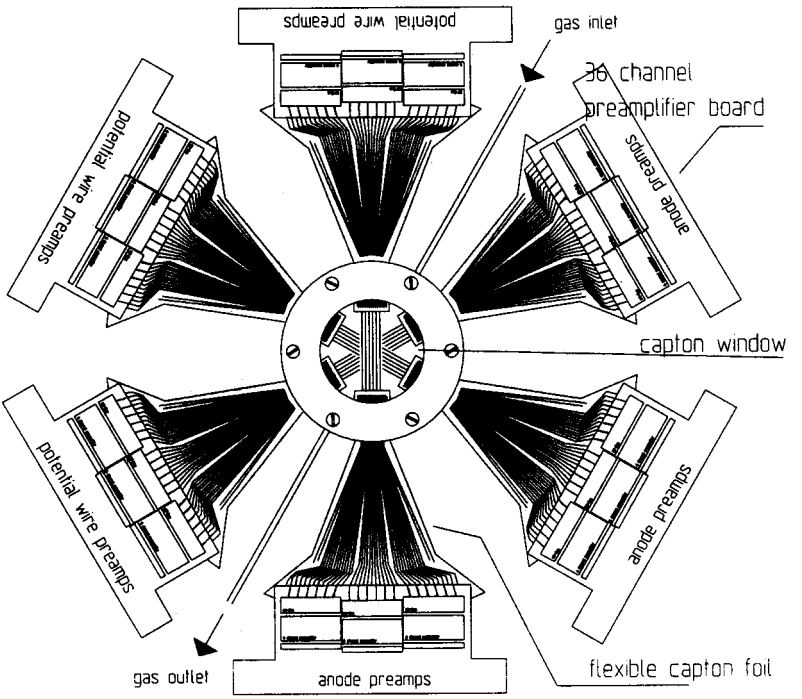

Fig. 2. Induction drift chamber

Due to the extremely narrow wire distances, the primary beam can pass the chamber with up to 10^7 protons per second [4].

Plans exist for the future development to build a chamber cylindrically around a very thin beampipe, so proton beams up to the highest COSY intensity are possible [Fig. 3].

This detector has an ideal detection possibility for secondary vertices, which in the COSY energy range are a sign for strangeness. It even offers a possibility to trigger on these events.

3. The fusion reaction $pd \rightarrow {}^3\mathrm{He}\,\eta$

It has been found at Saturne that this reaction has a surprisingly high cross-section (range of microbarns) [5]. This lead to new calculations and assumptions on the nature of this process.

Laget and Lecolley described the formation of ^{3}He with the η production by a three body mechanism [6], where each nucleon participates in a meson scattering process. There are new data points which indicate a flat behavior near to the threshold [7], leading to speculations on a bound η-nucleon state. The newest analysis comes from C. Wilkin [8], he concentrates on the

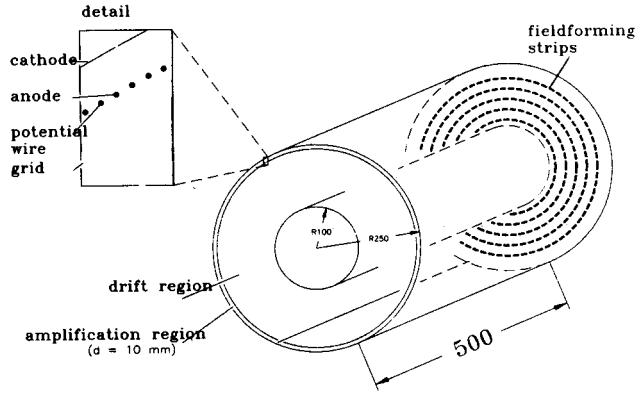

Fig. 3. Cylindrical drift chamber

threshold region. An amplitude $f(\eta)$ is extracted from the cross-section to be independent from phase space. The energy dependence of this amplitude is calculated assuming a strong final state interaction between the η and the ^{3}He. In addition a very weak angular dependence of the amplitude compared to the π^0 fusion reaction is found. This is a consequence of the s-wave dominance by the S_{11} - resonance in contrast to the p-wave resonance in π fusion.

The $dp \rightarrow {}^3He\,\eta$ reaction has become famous by the dominant peak in the so called threshold excitation curve of Saturne [9]. This dominant peak and the high count rate near to the threshold is explained by Kilian [10] with an accidental coincidence of two kinematic effects: the two step reaction and the velocity matching. This describes also the energy dependence of the cross section. An intermediate pion acts as a beam particle for the η production. The fusion probability of d+p to ^{3}He is then given by the relative energy of the d p system, *i.e.* the matching of their velocities.

The situation of measured data is shown in Fig. 4.

There are mainly two domains: An excitation measurement from the threshold to the maximum Saturne momentum from 0 to 6 degrees (lab. angle of ^{3}He) and a total cross-section measurement near production threshold. The region of expected measurements at CELSIUS is shown by the dotted area.

To investigate how we can extend the data with the first part of the TOF — spectrometer, this is a quirl and a ring, the lab-momentum distribution of the ^{3}He is plotted for different beam momenta [Fig. 5]. If the p_T axis is read as the height of the detector, the p_L axis can be taken as the distance between the detector and target, measured in m. This demonstrates how the distance for each beam momentum is optimized in order to get the best

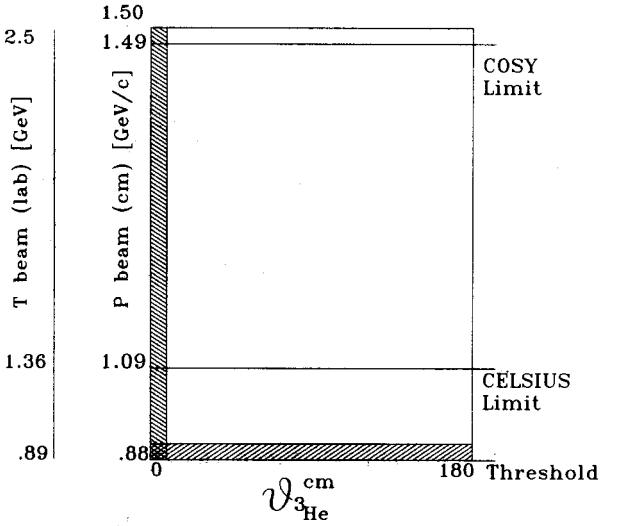

P. Berthet et al NUCL PHYS A443 (1985) 589

E. Chiavassa et al NUCL. PHYS. A519 (1990) 413c

A. Boudard et al PHYS LETT B214 (1988) 6

J. Berger et al PHYS REV LETT 61 (1988) 919

Fig. 4. Measured cross-section of $pd \rightarrow {}^3\mathrm{He}\,\eta$

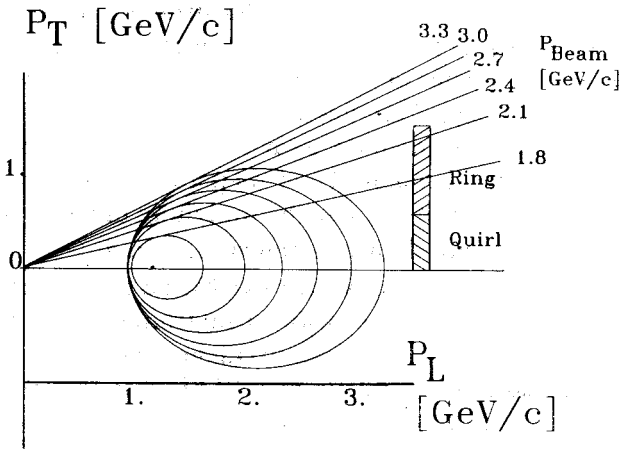

Fig. 5. Lab. momentum distribution of ^{3}He for different beam momenta

resolution with a 4π acceptance.

For a given time of flight resolution (assumed $\sigma(\Delta t) = 0.5$ nsec) the

momentum resolution is calculated for each beam-momentum:

$$\frac{\Delta p}{p} = \gamma^2 \cdot \frac{\Delta t}{t}.$$

The momentum resolution can be translated into the missing mass resolution: [Fig. 6].

$$\Delta M_x = \left(p_b \cdot cos(\theta) - \frac{E_t + E_b}{E_{^3He}} \cdot p_{^3He} \right) \cdot \frac{\Delta p}{M_x}.$$

(All quantities are in the Lab-system, E is the total energy, p the momentum, the indices b and t mark the beam and the target particle)

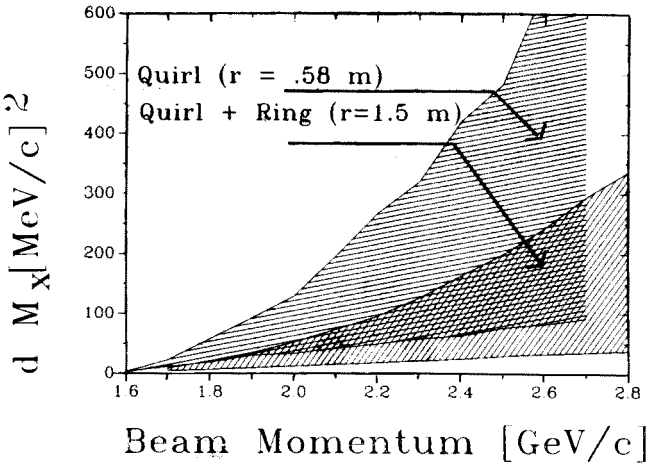

Fig. 6. Limits of missing mass resolution

This calculation gives of course only a lower limit of the errors in the missing mass as effects like multiple scattering *etc.* have to be added.

For a lower beam momentum Monte Carlo Calculations have been performed, they show that the ^{3}He can be very well separated from other particles especially from the Triton [11].

4. The fundamental reaction $pp \to pp\eta(\eta')$

This reaction is more complicated compared to the fusion measurement, as one has to detect two particles which do not have such a dominant behavior in dE/dx and time of flight as the ^{3}He due to its double charge and high mass.

The reaction is calculated by several authors: The analysis of Laget [12] is explained by the Feynman–Diagram [Fig. 7], the interactions marked

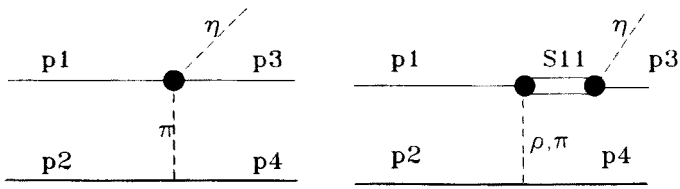

Fig. 7. Feynman graph for the calculation of $pp \to pp\eta$ [12].

with circles are related to measured data of $\pi N \to \eta N$. It is shown that the ρ exchange is dominant.

The scarce data, there are only three points stemming from bubble chamber experiments, do not allow the calculation to be tested precisely. The calculation of Liu *et al.* can be found in these proceedings.

The analysis of Germond and Wilkins [13] concentrates again on the threshold region. The graph in Fig. 8 represents the method of the calculation. Near to the threshold the final state interaction dominates the amplitude. Only the graph with the S_{11} resonance is taken into account, the excitation of the S_{11} is found to be dominated by the ρ exchange.

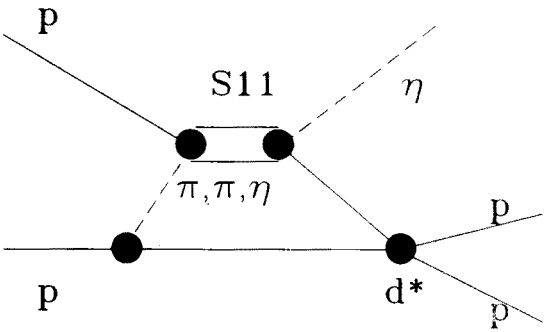

Fig. 8. Feynman graph for the calculation of $pp \to pp\eta$ [13].

New measurements from Saturne [14] seem to give cross sections much lower compared to the calculations.

The following Monte Carlo (Geant) results were calculated by assuming a fully equipped Time of Flight Spectrometer (7.5 m length and 1.5 m radius) The time resolution of start and stop counters is assumed to be $\sigma = 0.25$ nsec. The beam momentum is 2.4 GeV/c. The background is taken as $pp \to pp\,2\cdot\pi^0$ with a four times higher rate and $pp \to pp\,3\cdot\pi$ with the same rate as $pp \to pp\eta$. All effects such as straggling, decay, beamsize, hadronic interaction and production of secondary tracks are included. The η is identified in the missing mass spectrum of the scattered protons, this includes the combination background, where for example a pion from the η decay is mixed up with a scattered proton [Fig. 9].

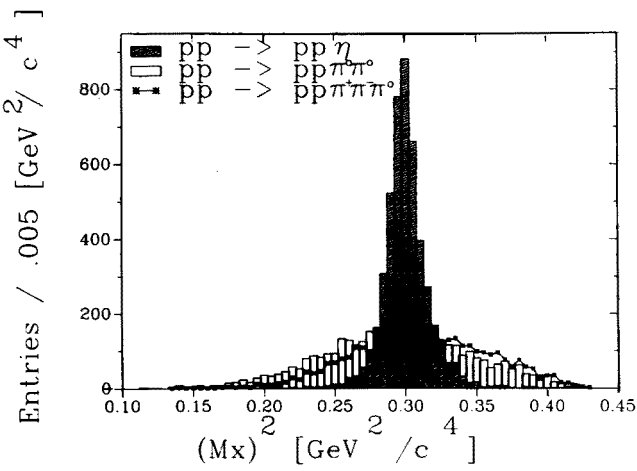

Fig. 9. Squared missing mass resolution of the η (beam momentum: 2.4 GeV/c)

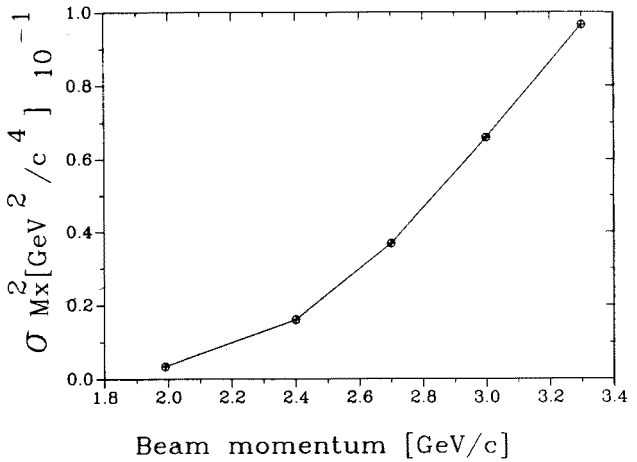

Fig. 10. Resolution of the squared missing mass distribution dependant on the beam momentum.

Kinematical constraints offer possibilities to cut off a lot of the combination background. Cuts can be set for example in the sum of the proton momenta, the scattering angle, the correlation between the two scattering angles, and the limits of the Dalitz-plot.

The measurement has the best resolution near to the threshold and gets worse for higher energies as shown in Fig. 10.

To improve the resolution at higher energies it is possible to use the charged decay mode of the η to reconstruct it in a second independent missing mass plot.

5. η and η' interaction

This measurement aims to give a contribution to the determination of the quark content of the η and η'. Following the notation of Rosner [15] the quark content of the pseudo scalar mesons can be plotted in the frame with the axes of nonstrange quark content and strange quark content. The solution has to be a point on the unitary circle (if there are no glueball or $c\bar{c}$ admixtures). Constraints are plotted which are calculated from different decays involving the η and η'. In case of the η', constraints for the strange axis are missing. The upper limit of the decay $\phi \to \eta' + \gamma$ is still to high [Fig. 11].

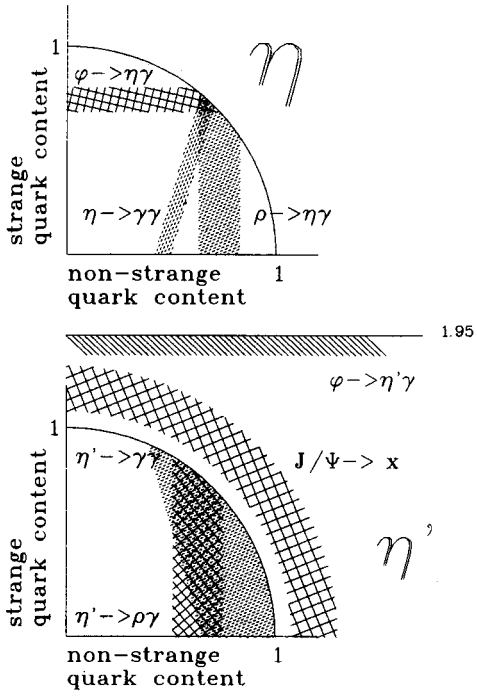

Fig. 11. Quark content of η and η' [15].

In principle the ratio of strange to nonstrange quark content of the η (η') could be deduced from the η, η' decay width into Kaon channels compared to pion channels. Of course the decay into Kaons is not allowed due to the lower mass of the η (η'). But instead of looking to the decay channels we can investigate the η (η') nucleon interaction channels. The measurement is explained with the graph in Fig. 12.

The task will be to reconstruct the η (η') mass from the interaction

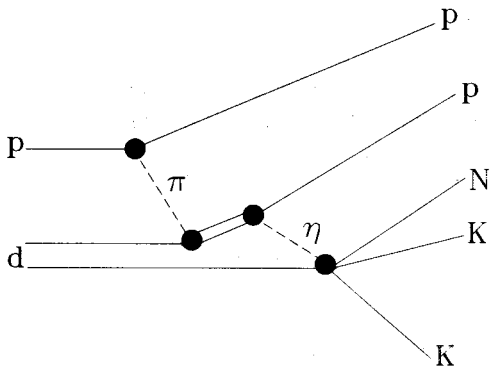

Fig. 12. η-N interaction

Range of η , η'

$$c\tau_0\gamma\beta\ (\eta) = 4 \cdot 10^{5}\ \text{fm}$$

$$c\tau_0\gamma\beta\ (\eta') = 5 \cdot 10^{2}\ \text{fm}$$

η	η'
pp->pp η n ↳ $K_s^o \Lambda$ ↳ $K^+ \Sigma^-$ ↳ $K_s^o K^- p$ ↳ $K_s^o K_s^o$ n	pp->pp η' n ↳ $K_s^o \Lambda$ ↳ $K^+ \Sigma^-$ ↳ $K_s^o K^- p$ ↳ $K_s^o K_s^o$ n
pp->pp η n ↳ $\pi^- p$	pp->pp η' n ↳ $\pi^- p$

STRANGE NON-STRANGE

pd->d ηn

Fig. 13. η, η' range and interaction channels

channel. The graph shows that this idea is related to the two step mechanism [10].

The η (η') is produced on a nucleon of the deuterium, the second nucleon is regarded as a spectator. The lifetime of the η and η' is long enough to correspond to a range which is much larger than the deuteron radius.

The channels which can be measured are shown in Fig. 13, the strange

particles will be detected by their secondary vertex.

As an absolute measurement of this complicated reaction is difficult we will measure the relative quantities given by the ratios of

$(\eta \to \text{strange})/(\eta \to \text{nonstrange})$, $(\eta' \to \text{strange})/(\eta' \to \text{nonstrange})$ and crossed values.

REFERENCES

[1] D. Grzonka, W. Oelert KFA-IKP(I) 1993-1.
[2] W. Borgs *et al.*, COSY E8 Proposal (1991).
[3] H. Machner *et al.*, Cosy Letter of Intent 24 (1992).
[4] E. Roderburg *et al.*, *Nucl. Instr. and Meth.* **A323**, 140 (1992).
[5] J. Berger *et al.*, *Phys. Rev. Lett.* **61**, 919 (1988).
[6] J.M. Laget, J.F. Lecolley, *Phys. Rev. Lett.* **61**, 2069 (1988).
[7] R.S. Kessler PhD Thesis UCLA (1992).
[8] C. Wilkin, *Phys. Rev.* **C47**, 938 (1993).
[9] F. Plouin, *Proc. Workshop on Production and Decay of Light Mesons*, ed. P. Fleury, World Scientific, Singapore, Paris 1988, p. 114.
[10] K. Kilian, H. Nann, KFA - IKP(I) 1991-1.
[11] R. Stratmann, private communications.
[12] J.M. Laget, F. Wellers, J.F Lecolley, *Phys. Lett.* **B257**, 254 (1991).
[13] J.F. Germond, C. Wilkin, *Nucl. Phys.* **A518**, 308 (1990).
[14] A.M. Berthold *et al.*, Preprint Centre de Recherches Nucleaire, University of Strasbourg, 1993.
[15] J.L. Rosner, *Phys. Rev.* **27D**, 1101 (1983).